Redox Gene Regulator Rex Divert Fermentation In Concert with Low Charge Export in *Streptococcus mutans*.

Authors: Divya Naradasu[1†], Takano Sotaro[1†], Shu Zhang[2], Toshinori Okinaga[3], Tatsuji Nishihara[4], Kenneth H. Nealson[5], Akihiro Okamoto[1,6,7*]

Affiliations:

[1] International Center for Materials Nanoarchitectonics, National Institute for Materials Science, 1-1 Namiki, Tsukuba, Ibaraki 305-0044, Japan.
[2] Interfacial Energy Conversion Group, National Institute for Materials Science, 1-1 Namiki, Tsukuba, Ibaraki 305-0044, Japan.
[3] Department of Bacteriology, Osaka Dental University, 8-1 Kuzuha-hanazano-cho, Hirakata-city, Osaka, 573-1121, Japan.
[4] Division of Infections and Molecular Biology, Department of Health Promotion, Science of Health Improvement, Kyushu Dental University, 2-6-1 Manazuru, Kokurakita-ku, Kitakyushu, 803-8580, Japan.
[5] Department of Earth Sciences, University of Southern California, Los Angeles, CA 90089, U.S.A.
[6] Center for Sensor and Actuator Material, National Institute for Materials Science, 1-1 Namiki, Tsukuba, Ibaraki 305-0044, Japan.
[7] Graduate School of Chemical Sciences and Engineering, Hokkaido University, 5-8, Jonishi, Kita Ward, Sapporo, Hokkaido 060-0808, Japan.

*Corresponding author. E-mail: OKAMOTO.Akihiro@nims.go.jp

† Authors equally contributed to the study.

This file includes:

Supplementary figures

Supplementary Fig. 1. Scanning electron microscope image of *S. mutans* cells attached on the electrode surface.
Supplementary Fig. 2. Quantification of riboflavin reduced, and charge transported by *S. mutans* in the presence of glucose in an anaerobic cuvette.
Supplementary Fig. 3. Evidences for direct electron transfer by *S. mutans*
Supplementary Fig. 4. Efflux changes in ethanol and L-lactate when altering the flux of key metabolic reactions.
Supplementary Fig. 5. Effect of labeled $^{15}NH_4Cl$ on current production of *S. mutans.*
Supplementary Fig. 6. Time course of the electrolyte pH during the electrochemical operations.
Supplementary Fig. 7. High sensitivity of Rex to NAD^+ generation in *S. mutans.*

Supplementary tables

Supplementary Table. 1. List of differentially expressed genes associated with metabolism in electrode attached *S. mutans* under SA vs OCV conditions with fold change 1.5.
Supplementary Table. 2. Assimilation of ^{15}N% (ratio of ^{15}N to total nitrogen) in *S. mutans* wild type (WT) and Δ*rex* under single-potential amperometry (SA) and open circuit voltage (OCV) conditions with and without riboflavin (RF).
Supplementary Table. 3. Percentage of cells with low ^{15}N% incorporation (<10%) in *S. mutans* wild type (WT) and Δ*rex* under single-potential amperometry (SA) and open circuit voltage (OCV) conditions without/with riboflavin (RF).
Supplementary Table. 4. List of differentially expressed genes associated with metabolism of *S. mutans* wild type (WT) and *rex* mutant with fold change 1.5.
Supplementary Table. 5. List of EET-capable bacteria, their potential EET mechanism and their gene names assigned as redox regulator Rex in the database of National Center for Biotechnology Information.
Supplementary Table. 6. List of amino acid sequence of Rossman-like folding identified by the Cofactory v.1.0 and their length.

Supplementary text

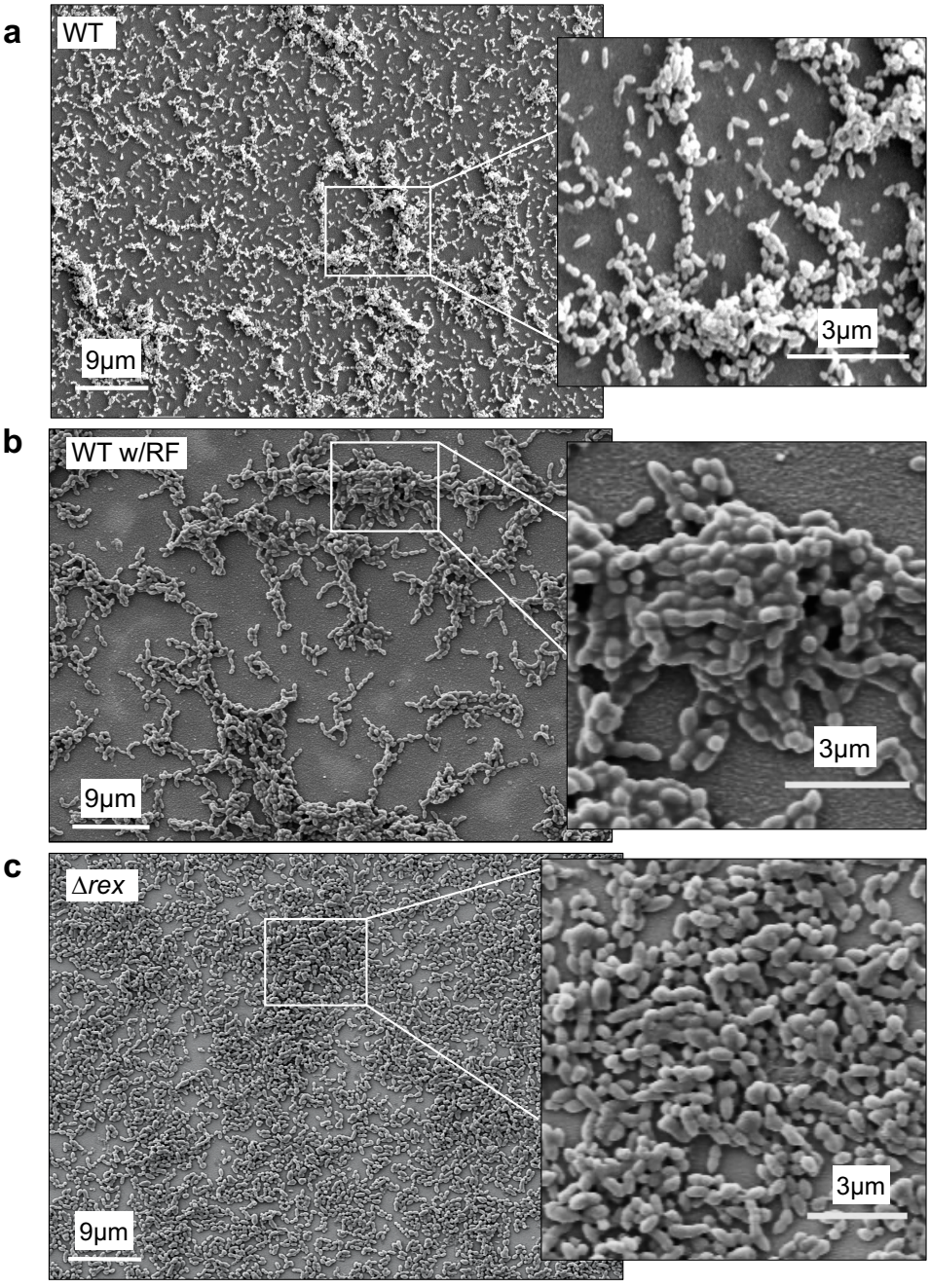

Supplementary Fig. 1 | Scanning electron microscope images of *S. mutans* cells attached on the electrode surface. a) *S. mutans* WT **b)** WT in the presence of riboflavin (RF) and **c)** Rex deleted *S. mutans* **(**Δ*rex*) after 24 hours of current production with 10 mM glucose at +0.4 V (versus SHE), cells were intact on the electrode surface.

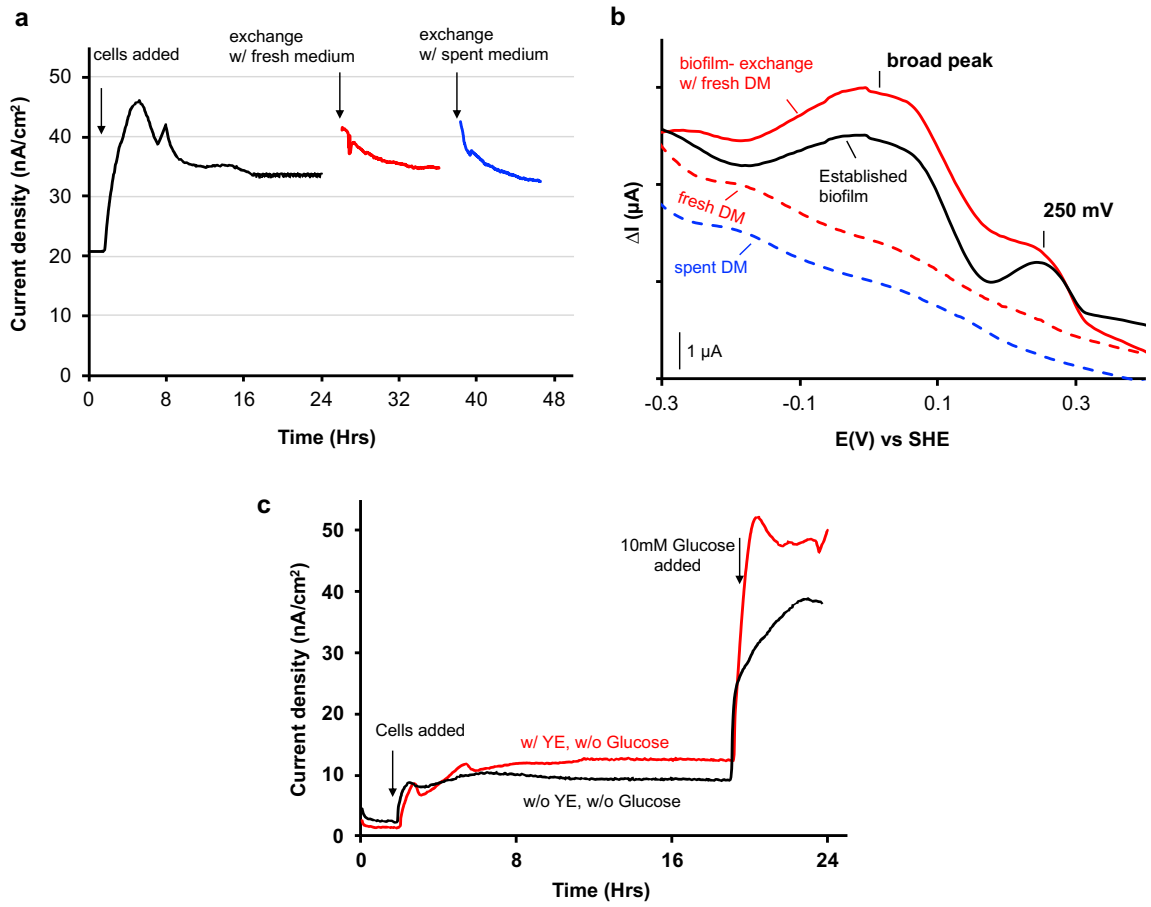

Supplementary Fig. 2 | Evidences for direct electron transfer by *S. mutans*. a) Supernatant replacement during the current production of *S. mutans* at +0.4 V (versus SHE). At the indicated times, the medium was removed and replaced with sterile defined medium containing 10 mM glucose (red line) or cell free spent medium (blue line), leading to no decrease in current production. The same tendency was confirmed in three individual experiments. **b)** Baseline-subtracted differential pulse voltammograms in the presence of *S. mutans* before (black solid line) and after medium exchange (red solid line). Data for sterile DM (red dotted line) and cell free spent medium (blue dotted line) are also represented. **c)** Effect of the removal of yeast extract (YE) on the current production of *S. mutans*. In the absence of YE, the glucose oxidation current production after the addition of 10 mM glucose reached to the value approximately 15 % smaller than that in the presence of YE. Because YE provides essential nutrients for protein synthesis, a little less current production is explainable by not only shuttling of riboflavin contained in the YE but also less cellular protein synthesis for direct electron transport mechanism.

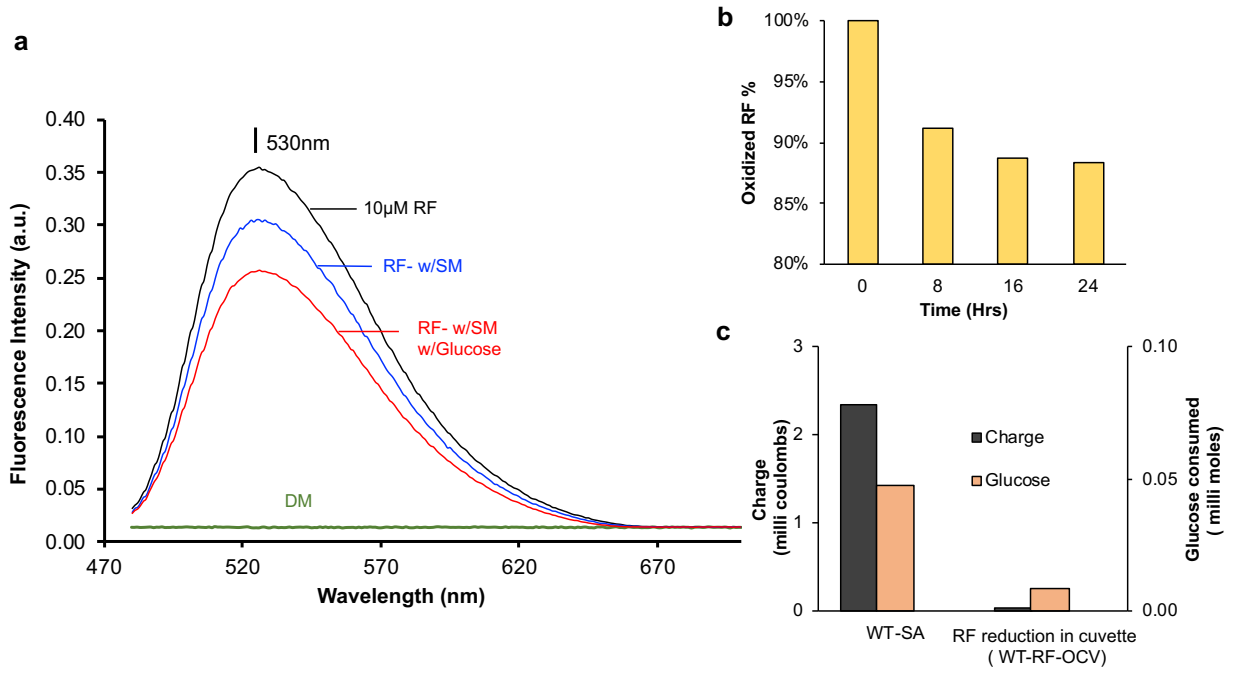

Supplementary Fig. 3 | Quantification of reduced riboflavin, and charge transported by *S. mutans* in the presence of glucose in an anaerobic cuvette. **(a)** Emission spectrum of oxidized riboflavin (RF) measured by excitation at 450 nm, showing the fluorescence intensity peak of 10 μM RF (black line) at 530 nm. Upon the addition of *S. mutans* (SM) to 3 mL of deaerated DM at $OD_{600} = 0.1$ (blue line), and subsequent addition of 10 mM glucose. **(b)** The time course of oxidized RF fluorescence intensity (red line) in cuvette measured at every 8 hours. **(c)** The graph showing the charge estimated from RF reduction and amount of glucose consumed after 24 hours in the cuvette, from which we estimated the columbic efficiency in the open circuit condition with SM in the presence of RF (WT-RF-OCV) in Figure 3A.

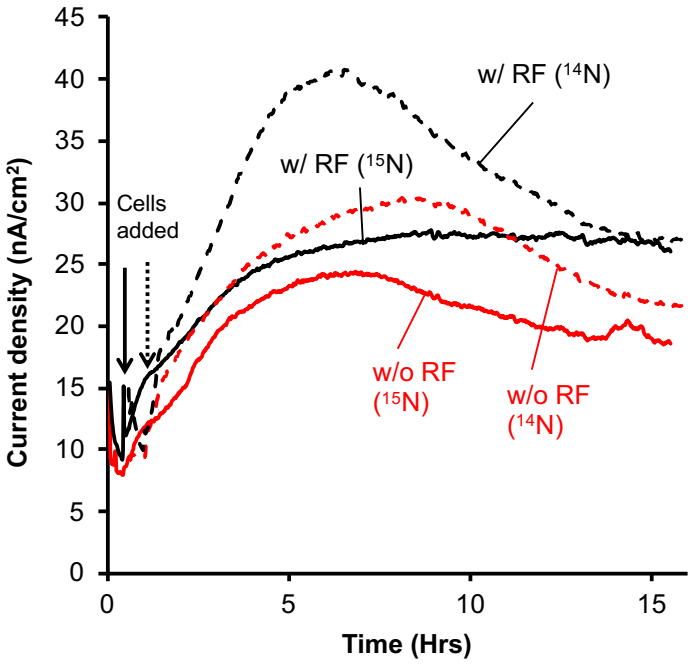

Supplementary Fig. 4 | Effect of labeled $^{15}NH_4Cl$ on current production of *S. mutans*. Current production of *S. mutans* vs. time measurements conducted in anaerobic reactor equipped with ITO electrodes (surface area: 3.14 cm^2) poised at +0.4 V (versus SHE) containing DM with labeled and unlabeled NH_4Cl as sole N source in the presence and absence of 10 μM riboflavin (RF) with 10 mM glucose. The solid and dotted arrows indicate the timing of cell addition to the reactor with ^{15}N and ^{14}N labeled medium, respectively.

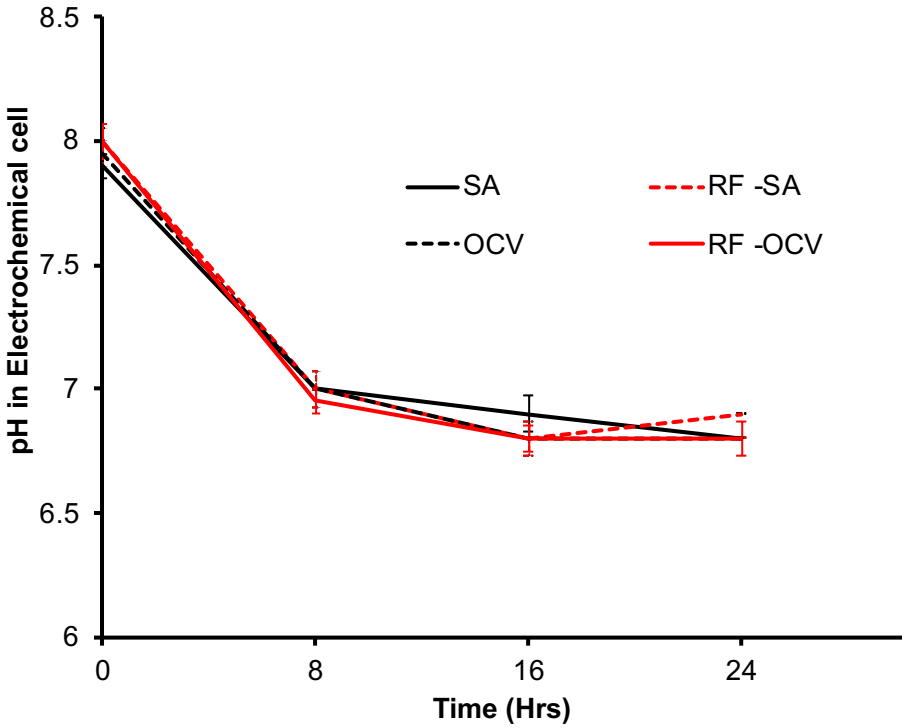

Supplementary Fig. 5 | Time course of the electrolyte pH during the electrochemical operations under single-potential amperometry (SA) and open circuit voltage (OCV) conditions in the presence and absence of riboflavin (RF). We measured pH at every 8-hour time interval during the electrochemical measurement. The data shown are mean values ± standard deviations of two individual experiments.

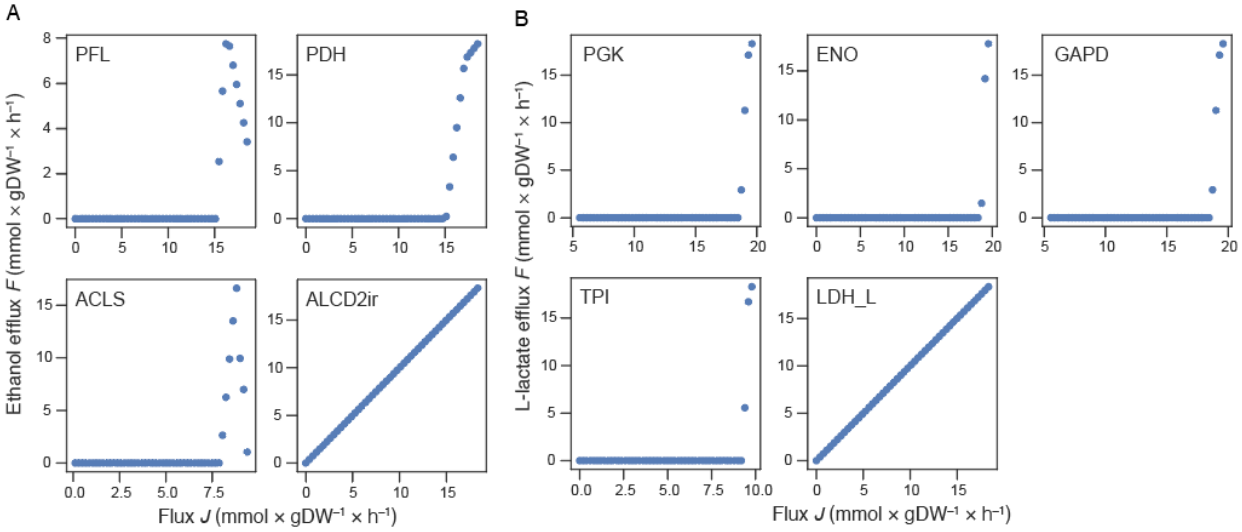

Supplementary Fig. 6 | Efflux changes in ethanol and L-lactate when altering the flux of key metabolic reactions. (a) Changes in efflux of ethanol by altering a flux in pyruvate formate-lyase (PFL), pyruvate dehydrogenase (PDHcr), acetolactate synthase (ACLS) or alcohol dehydrogenase (ALCD2ir) from its lower to upper limit. **(b)** Changes in L-lactate efflux by altering a flux in phosphorglycerate kinase (PGK), enolase (ENO), glyceraldehyde-3-phosphate dehydrogenase (GAPD), triose-phosphate isomerase (TPI) or L-lactate dehydrogenase (LDH_L) from its lower to upper limit. *J* and *F* corresponds to those in Fig. 4A.

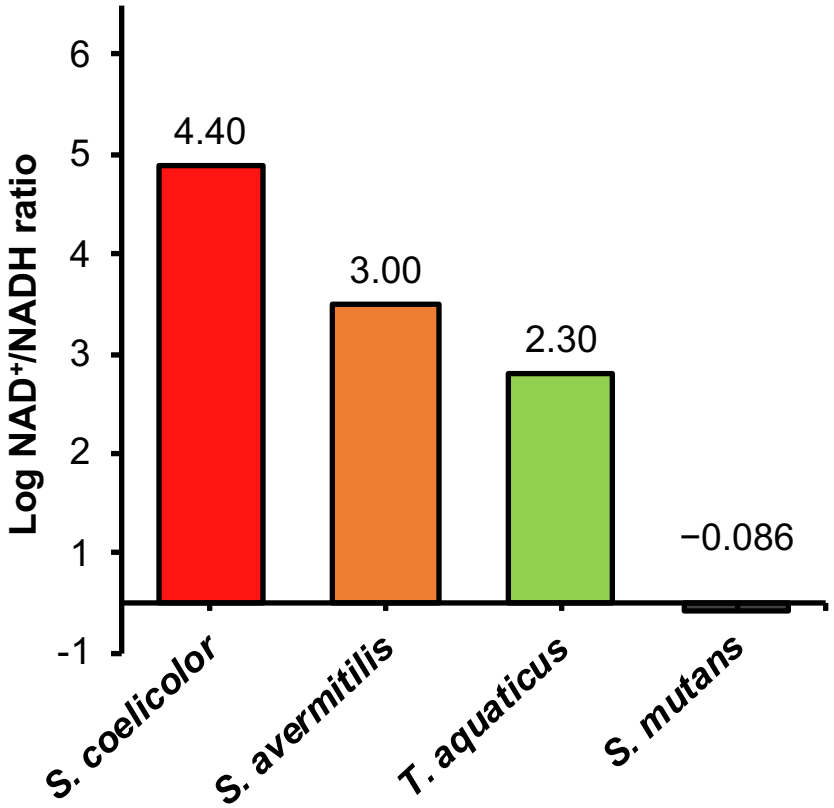

Supplementary Fig. 7 | High sensitivity of Rex to NAD^+ generation in *S. mutans.* The minimum logarithmic NAD^+/NADH ratio to form 100% Rex–DNA complexes in *S. mutans* determined by the amount of glucose consumed and lactate produced (See supplementary text). Data for *S. coelicolor, S. avermitilis,* and *T. aquaticus* were from references 36,37,38.

Supplementary Table. 1 | Assimilation of ^{15}N% (ratio of ^{15}N to total nitrogen) in *S. mutans* wild type (WT) and Δ*rex* under single-potential amperometry (SA) and open circuit voltage (OCV) conditions with and without riboflavin (RF). The data shown are the concurrent results of two individual experiments with standard errors of means (SEM).

$^{15}N/N_{total}$ (%)		
Condition (total number of cells)	Mean%	SEM%
WT-OCV (n=231)	13	0.46
WT-SA(n=209)	16.44	0.36
WT RF-OCV(n=220)	13.82	0.28
WT RF-SA(n=216)	13.01	0.24
Δ*rex*-OCV(n=200)	10.92	0.4
Δ*rex*-SA (n=200)	9.42	0.3

Supplementary Table. 2 | Percentage of cells with low ^{15}N% incorporation (<10%) in *S. mutans* wild type (WT) and Δ*rex* under single-potential amperometry (SA) and open circuit voltage (OCV) conditions without/with riboflavin (RF).

Condition (total number of cells)	No of low active cells <10%	% of low active cells to total no of cells
WT-OCV (n=231)	83	42%
WT-SA(n=209)	8	4%
WT RF-OCV(n=220)	45	23%
WT RF-SA(n=216)	25	13%
Δ*rex*-OCV(n=200)	95	47.5%
Δ*rex*-SA (n=200)	92	46%

Supplementary Table. 5 | List of EET-capable bacteria and Archaea, their potential EET mechanism and their gene names assigned as redox regulator Rex in the database of National Center for Biotechnology Information.

EET mechanism	Organism	*rex* Gene name
Flavin based complex	*Streptococcus dysgalactiae*	SDSE_0916
	Granulicatella elegans	HMPREF0446_01247
	Trichococcus pasteurii	TPAS_2663
	Pisciglobus halotolerans	SAMN04489868_12010
	Alkalibacterium gilvum	SAMN04488113_13626
	Lactococcus lactis	LL1060
	Lactococcus garvieae	LCGL_1020
	Bacillus circulans	C2I06_21170
	Caldanaerobius fijiensis	SAMN02746089_00712
	mahella australiensis	Mahau_0374
	Clostridium intestinale	CINTURNW_0232
	Romboutsia weinsteinii	CHL78_017725
	Cellulosilyticum lentocellum	Clole_3033
	Faecalibacterium prausnitzii	FPR_01980
	Streptococcus suis	SSGZ1_0943
	Clostridium botulinum	CBO3306
	Eremococcus coleocola	HMPREF9257_0586
	Oenococcus oeni	OEOE_1398
	Carnobacterium maltaromaticum	BN424_1284
	Lactobacillus plantarum	lp_0725
	Vagococcus lutrae	T233_01518
	Enterococcus saccharolyticus	OMQ_00682
	Enterococcus faecalis	EF_2638
	Enterococcus faecium	A5810_002288
	Listeria Monocytogenes	LMOf2365_2104
Cytochrome mediated EET	*Thermincola potens*	TherJR_2553
Fermentation associated EET	*Enterococcus avium*	OMU_04218
	Klebsiella pneumoniae	BU230_13650
Cytochrome mediated EET in *Archaea*	*Methanosarcinales archaeon*	DRN98_10615

Supplementary Table. 6 | List of amino acid sequence of Rossman-like folding identified by Cofactory v.1.0 and their length.

Rossman like folding sequence identified by Cofactory v.1.0	Sequence length
>*Streptomyces coelicolor* QDWPVVIVGIGNLGAALANYGGFASRGFRVAALIDADPGMAGKP	44
>*Streptomyces avermitilis* QDWPVVIVGIGNLGAALANYGGFASRGFRVAALIDADPAMAGKPV	45
>*Thermus aquaticus* WGLCIVGMGRLGSALADYPGFGESFELRGFFDVDPEKVGR	37
>*Klebsiella pneumoniae* ITRVALIGVGNLGTAFLHYNFTKNNNTKIEMAFDVSEE	35
>*Faecalibacterium prausnitzii* TILIGCGRLGKAVSRFITTDTNGYKLIAAFDVAENEVGKEISGI	41
>*Streptococcus mutans* STTNVLLVGVGNIGRALLNYRFHERNKMKIAMAFDTDDNEQVGQ	41
>*Streptococcus suis* ITNVMLVGVGNMGRALLHYRFHERNKMKIVMAFEADDNPA	37
>*Enterococcus avium* QLTNVALVGVGNLGSALLKFKFHQSNSIRVSCAFDVKE	35
>*Enterococcus faecium* QLTNVALIGVGNLGSALLKYKFHQSNSIRISCAFDVNEEIVG	39
>*Enterococcus saccharolyticus* QMTNVALIGVGNLGSALLKYKFHQSNSIRVSAAFDVNPDI	37
>*Enterococcus faecalis* EEKRIALIGCGNLGKALLKNNFRRNENLNIVCAFDNDSALVGTT	41
>*Vagococcus lutrae* RLTNVALIGVGNLGNALLNYGFHQGNNIRISAAFDVKED	36
>*Listeria monocytogenes* KQTNVALIGVGNLGTALLHYNFMKNNNIKIVAAFDVDPAKVGSVQQ	43
>*Eremococcus coleocola* RLTSVGLVGVGNLGNALLNYNFRKNHNIRISAGFDINPEIVGTIHS	43
>*Lactobacillus plantarum* LTNVALIGVGNLGHALLNFNFHKNSNVRISAAFDVNEAIANTVQS	42
>*Oenococcus oeni* KLNKVAVVGTGNLGQALMKYNFVHSSNIQIVMGFDVDPKKKELKI	42
>*Clostridium botulinum* NPYNIIIIGAGNIGQALANYTRFSKLGFNVKAMFDTNPKLIGL	40
>*Cellulosilyticum lentocellum* QNYKMIIVGVGNLGQAIANSTSFSKRGFKLIGLFDVNPRLIGMS	41
>*Romboutsia weinsteinii* SYNAILVGAGNLGQAIANYSGFRKAGFEIKALFDANPKMIGL	39

Supplementary Text:

As described in Figure 5A, the NADH redox sensor Rex represses the transcription of pyruvate dehydrogenase upon sensing a NAD^+/NADH ratio and Rex-DNA complex formation, resulted in the suppression and enhancement of the ethanol and lactate production, respectively. In our SA conditions, we detected significant amount of lactate but no ethanol as an end product. Therefore, we assumed that 100% activation of Rex-DNA complex formation in the SA conditions of *S. mutans,* and approximated the intracellular NAD^+/NADH ratio that corresponds to 100% activation of Rex-DNA complex formation by using lactate and glucose concentration at 8, 16, and 24 hour in our SA conditions in the presence or absence of RF. Eight hour data in the presence of riboflavin gave the minimum value of -0.09 among calculated logarithmic NAD^+/NADH ratios (Supplementary Fig. 7). We then compared the ratio with those corresponding to 100% activation of Rex-DNA complex in purified Rex proteins from *S. coelicolor, S. avermitilis*, and *T. aquaticus* (references 36,37,38).